

Supporting Information

Anthracene-[1]benzothieno[3,2-b][1]benzothiophene (BTBT) dyad and triads as p-type semiconductors for organic field-effect transistors and phototransistors

Maowei Qi,^{1‡} Dongwei Zhang^{1,4*‡}, Yanan Zhu³, Changbin Zhao², Aiyuan Li², Fobao Huang,^{1,4} Yaowu He^{2*} & Hong Meng^{1,2*}

¹ School of Microelectronics, Northwestern Polytechnical University, Xi'an 710072, China

² School of Advanced Materials, Peking University Shenzhen Graduate School, Shenzhen 518055, China

³ Faculty of Materials Science, Shenzhen MSU-BIT University, Shenzhen, 518172, China

⁴ Yangtze River Delta Research Institute of NPU, Taicang, No. 27 Zigang Road, Science and Education New Town, Taicang, Jiangsu, 215400, China.

*Corresponding Authors: zhangdw@nwpu.edu.cn; hyw@pku.edu.cn; menghong@pku.edu.cn.

‡ These authors contributed equally to this work.

Experimental

Chemicals and Instruments

All the solvents and commercial chemicals (**1**, **4**, **8**, **10**) were purchased from Energy Chemical Co. and were used as received without further purification. ^1H and ^{13}C NMR spectra of soluble intermediates were recorded on a Bruker DRX NMR spectrometer operating at 300 MHz (for ^1H NMR) and 75 MHz (for ^{13}C NMR) in chloroform-*d* solutions. MALDI-TOF mass-spectra were recorded on a Bruker MALDI Autoflex Speed mass spectrometer. Elemental analyses were performed on ELEMENTAR vario EL cube EA-01 analyzer. Purification of the final compounds was done by vacuum sublimation on a 5-zone furnace BTF-1200C-V under high vacuum ($\sim 10^{-2}$ mbar).

Synthesis

Intermediates **BTBT** (**2**),^[1] **2-bromo-BTBT**(**3**),^[2] **2,7-dibromo-BTBT** (**7**),^[3] 2-(anthracen-2-yl)-4,4,5,5-tetramethyl-1,3,2-dioxaborolane (**9**),^[4] 2,6-bis(4,4,5,5-tetramethyl-1,3,2-dioxaborolan-2-yl)-anthracene (**11**),^[4] were synthesized according to the literature procedures.

The target compounds **An-BTBT**, **An-BTBT-An** and **BTBT-An-BTBT** are very insoluble materials. We were unable to record their NMR spectra due to their very low solubility, so the compounds were characterized by MS, elemental analyses and single crystal X-ray diffraction.

2-(Anthracen-2-yl)benzo[*b*]benzo[4,5]thieno[2,3-*d*]thiophene (An-BTBT). 2-(Anthracen-2-yl)-4,4,5,5-tetramethyl-1,3,2-dioxaborolane (**9**) (3.04 g, 10.0 mmol) and 2-bromo-BTBT (**3**) (3.80 g, 12.0 mmol) were added to a 350 mL high-pressure reaction bottle charged with degassed toluene (100 mL). A nitrogen degassed 2.0 M aqueous solution of K_2CO_3 (25 mL, 50 mmol) was added to the suspension. Then the phase-transfer agent Aliquat[®]336 (1.0 mL) was added and the mixture was stirred under nitrogen for 15 minutes. After that, the catalyst tetrakis(triphenylphosphine)palladium (0), ($\text{Pd}(\text{PPh}_3)_4$) (0.231 g, 0.20 mmol) was added to the mixture and the mixture was heated to 95°C for 36 h under a nitrogen atmosphere. The mixture was cooled down to room temperature and the resulting solid was collected by filtration. It was consequently washed with methanol, diluted hydrochloric acid, water, acetone and chloroform. The crude product was further purified by sublimation twice in high vacuum ($\sim 5 \times 10^{-2}$ mbar) to afford pure compound **An-BTBT** (2.20 g, 45%) as a yellow solid.

MS (MALDI-TOF) *m/z*: 415.48 (M^+ , 100%). Calcd. for $\text{C}_{28}\text{H}_{16}\text{S}_2$: 416.07.

Anal. Calcd. for $\text{C}_{28}\text{H}_{16}\text{S}_2$: C, 80.74; H, 3.87; S, 15.39. Found C, 80.59; H, 3.97; S, 15.44.

2,6-Bis(benzo[*b*]benzo[4,5]thieno[2,3-*d*]thiophen-2-yl)anthracene (BTBT-An-BTBT). This compound was synthesized following the above procedure of Suzuki coupling, using 2,6-bis(4,4,5,5-tetramethyl-1,3,2-dioxaborolan-2-yl)-anthracene (**11**) (4.30 g, 10 mmol) and 2-bromo-BTBT (**3**) (8.00 g, 25 mmol), $\text{Pd}(\text{PPh}_3)_4$ (0.23g, 0.2mmol), Aliquat[®]336 (1.0 mL), 2 M K_2CO_3 (25 mL, 50 mmol) and toluene (100 mL). Yield: 1.83g (28%), bright yellow solid.

MS (MALDI-TOF) *m/z*: 654.19 (M^+ , 100%). Calcd. for $\text{C}_{42}\text{H}_{22}\text{S}_4$: 654.06.

Anal. Calcd. for $\text{C}_{42}\text{H}_{22}\text{S}_4$: C, 77.03; H, 3.39; S, 19.58. Found C, 77.16; H, 3.30; S, 19.35.

2,7-di(anthracen-2-yl)benzo[*b*]benzo[4,5]thieno[2,3-*d*]thiophene (An-BTTB-An). This compound was synthesized following the above procedure of Suzuki coupling, using 2-(anthracen-2-yl)-4,4,5,5-tetramethyl-1,3,2-dioxaborolane (**9**) (7.60 g, 25 mmol) and 2,7-

dibromo-BTBT (**7**) (4.00 g, 10mmol), Pd(PPh₃)₄ (0.23g, 0.20 mmol), Aliquat[®]336 (1.0 mL), 2 M K₂CO₃ (25 mL, 50 mmol) and toluene (100 mL). Yield: 2.00 g (35%), bright yellow solid. MS (MALDI-TOF) *m/z*: 591.48 (M⁺, 100%). Calcd. for C₄₂H₂₄S₂: 592.13. Anal. Calcd. for C₄₂H₂₄S₂: C, 85.10; H, 4.08; S, 10.82. Found C, 85.45; H, 4.02; S, 10.83.

Device fabrications and measurements

Surface modification of Si/SiO₂ substrates with OTS. We used prime grade highly doped n-type Si wafers with a 200nm thermally grown SiO₂ gate dielectric. These wafers were cleaned in piranha solution (7:3 mixture of H₂SO₄ and H₂O₂) for 30 min, rinsed with deionized water and dried under a nitrogen stream. For the surface modification, the wafer was treated with octadecyltrichlorsilane (OTS) by immersing the clean wafer substrate into 0.1 M solution of OTS in toluene at 60 °C for 30min to form self-assembled monolayer on the surface. The substrate was then rinsed with toluene and dried with nitrogen flow.

Device fabrications. The films of studied materials as the active layers of OFET were then deposited on the OTS-modified Si/SiO₂ substrates at various substrate temperatures (20, 60, 90 or 120 °C) by vacuum deposition under a pressure of 1×10⁻⁴ Pa. The semiconductor layer of 50 nm thickness was deposited over the treated surface through a shadow mask. Bottom gate top contact geometry of OFET was employed to measure the charge transport properties. The silicon served as the gate electrode. Gold films as the source and drain electrodes were thermally evaporated on the top of semiconductor layer through the shadow masks with typical channel length (L) and width (W) of L × W = 38 × 380 μm, 58 × 580 μm and 78 × 780 μm.

Testing OFET devices. The performances of fabricated OFETs were measured at room temperature under ambient conditions using Agilent 1500B semiconductor device parameter analyzer. The hole mobilities (μ_h) of OFETs were then extracted from the saturated regime using the relationship:

$$\mu_h^{\text{sat}} = (I_D \times 2L) / [W \times C \times (V_G - V_T)^2]$$

where I_D denotes the current between the drain and source, C is the capacitance per unit area of the modified SiO₂ gate insulator, V_G is the gate voltage, V_T is the threshold voltage, and W and L are the width and length of the conducting channel.^[5]

Growing single crystals and testing single crystal OFET devices. The single crystals were grown in a three-zone furnace via physical vapor transport (PVT) method. The temperatures in the furnace were set T₁ = 410 °C, T₂ = 310 °C and T₃ = 210 °C for growing **An-BTBT-An** crystals and T₁ = 450 °C, T₂ = 310 °C and T₃ = 200 °C. for growing **BTBT-An-BTBT** crystals. Single crystals were collected in the second zone. 300 nm SiO₂/Si substrates were put directly into the furnace to obtain the single crystals for device fabrication. The top contact bottom gate OFET devices were fabricated with ultrathin wire as shadow mask. Gold was evaporated as source and drain electrodes on the top of the crystal. The transfer and the output characteristics of single-crystal OFETs were obtained with B1500A semiconductor analyzer combined a probe station.

Phototransistor measurements. The photoresponsive characteristics were obtained with the monochromic light (380 nm) from LE-SP-MON1000THP-S28MSB as a light source. Photoswitching characteristics were measured using blue LED light source with a wavelength centered at 420 nm and a power of 10 mW cm⁻².

Instruments and Methods

Single Crystal X-ray Diffraction Crystallography

Single crystals of **An-BTBT** and **BTBT-An-BTBT** were grown by vapor deposition method. The data for single crystals of compounds **BTBT-An-BTBT** and **An-BTBT-An** were collected at 100 K on a Rigaku Oxford Diffraction Supernova Dual Source, Cu at Zero equipped with an AtlasS2 CCD using Cu K α radiation. Data reduction was carried out with the diffractometer's software.^[6] The structures were solved by direct methods using Olex2 software^[7] and the non-hydrogen atoms were located from the trial structure and then refined anisotropically with SHELXL-2014^[8] using a full-matrix least squares procedure based on F^2 . The weighted R factor, wR and goodness-of-fit S values were obtained based on F^2 . The hydrogen atom positions were fixed geometrically at the calculated distances and allowed to ride on their parent atoms. Crystallographic data for the structure reported in this paper have been deposited at the Cambridge Crystallographic Data Center and allocated with the deposition numbers: CCDC 1909445 and 1909446 for compounds **BTBT-An-BTBT** and **An-BTBT-An**, respectively. Single crystal X-ray structures of **An-BTBT** and **BTBT-An-BTBT** with short C \cdots H, S \cdots S, C \cdots S, S \cdots π . contacts are shown in Figures S3 and S4.

TGA and DSC

Thermogravimetric analysis (TGA) was carried out on a Perkin Elmer TGA7.TGA system at a heating rate of 10 °/min under nitrogen flow rate of 60 cm³/min. Differential scanning calorimetry (DSC) was run on a Netzsch calorimeter model Polyma DSC214 at a heating and cooling rates of 10 °/min under nitrogen flow.

UV-Vis absorption and photoluminescence spectroscopy

UV-Vis electron absorption spectra were recorded on Shimadzu UV-1750 U and Perkin-Elmer Lambda 750 spectrophotometers. The solution spectra were measured in 10 mm path length square quartz cells in tetrahydrofuran (Figure 2b). For **An-BTBT**, UV-Vis absorption spectra were also measured in chlorobenzene and chloroform (Figure S2). For the solid-state measurements, the samples were deposited on quartz plates by vacuum deposition under a pressure of 1×10^{-5} Pa.

Photoluminescence spectra were recorded on Hitachi F-4600 spectrofluorometer. The solution spectra were measured in 10 mm path length square quartz cells in tetrahydrofuran (Figure 2b). The samples were excited at $\lambda_{\text{exc}} = 332$ nm (**An-BTBT**), 298 nm (**An-BTBT-An**) or 295 nm (**BTBT-An-BTBT**). For the solid-state measurements, the samples were deposited on the quartz plates by vacuum deposition under a pressure of 1×10^{-5} Pa. The samples were excited at $\lambda_{\text{exc}} = 365$ nm (**An-BTBT** and **BTBT-An-BTBT**) or 350 nm (**An-BTBT-An**).

Cyclic voltammetry

Cyclic voltammetry experiments were performed using potentiostat-galvanostat, model CHI660E (CH Instruments Inc). The materials for CV studies were deposited on the working electrode by vacuum deposition under a pressure of 1×10^{-4} Pa. The measurements were performed by three-electrode scheme using glassy carbon as the working electrode (diameter 3 mm), Pt disk as the counter electrode, and non-aqueous Ag/Ag⁺ (Ag wire, 0.01 M AgNO₃ and 0.1 M Bu₄NPF₆ in acetonitrile) as the reference electrode. Cyclic voltammograms were recorded at room temperature in CH₃CN as the solvent with 0.1 M Bu₄NPF₆ as the supporting electrolyte. The measured potentials were calibrated with ferrocene as an internal reference, which showed potential of 0.080V (when measuring **An-BTBT**) or 0.084V vs. Ag/Ag⁺ pseudo-reference electrode (when

measuring **BTBT-An-BTBT** and **An-BTBT-An**). The HOMO energy levels were estimated according to equation:

$$E_{\text{HOMO}} = -(e \cdot E_{\text{ox}}^{\text{onset}} + 4.80) [\text{eV}],$$

where $E_{\text{ox}}^{\text{onset}}$ is the onset potential of the anodic oxidation of the studied compounds vs. Fc/Fc⁺ as an internal standard (strictly speaking, for small molecules in solution, the half-wave redox potentials $E_{\text{ox}}^{1/2}$ should be used in the above equation. Because of irreversibility of oxidation process, not allowing estimation of $E_{\text{ox}}^{1/2}$ half-wave potentials, we had to use onset potentials $E_{\text{ox}}^{\text{onset}}$ instead).

Thin-film and single-crystal XRD experiments

XRD patterns were recorded using a Bruker D8 Advance X-ray diffractometer with a Cu K α source ($\lambda = 1.541 \text{ \AA}$) operating at 30 kV and 20 mA with a copper target ($\lambda = 1.54 \text{ \AA}$) and at a scanning rate of 1 °/min. The thin films samples of all three compounds were vacuum deposited on the OTS-modified Si/SiO₂ substrates at different temperatures of the substrate (20, 60, 90 and 120 °C). The single crystals used for XRD analysis (and for testing in OFET devices) were grown in a three-zone furnace via physical vapor transport (PVT) method. The temperatures in the zones were set as T₁ = 410 °C, T₂ = 310 °C and T₃ = 210 °C for **An-BTBT-An** growth, and T₁ = 450 °C, T₂ = 310 °C and T₃ = 200 °C for **BTBT-An-BTBT** growth. 300 nm SiO₂/Si substrates were put directly into the furnace to obtain the single crystals.

AFM microscopy

AFM images of vacuum-deposited films were obtained using a Bruker MultiMode 8 AFM system in tapping mode with ScanAsyst[®]. The films were deposited on OTS-treated Si/SiO₂ substrates at 20 °C or at 90 °C as described below for fabrication of OFET devices.

Polarizing Optical Microscopy (POM)

The optical photographs of **An-BTBT-An** and **BTBT-An-BTBT** crystals grown by physical vapor transport (PVT) method were taken with CARL ZEISS Axio Scope.A1.

Computational Methodology

The computational studies were carried out using density functional theory (DFT) method with Gaussian 16 (v. 1.1) or Gaussian 09 (revision D.01) package of programs.^[9] The geometries were fully optimized for isolated molecules in a gas phase or in solvents (tetrahydrofuran or acetonitrile, using PCM model), with no constraints, using B3LYP gradient-corrected functional with 6-311G(d,p) basis set. Spin-restricted formalism was used for optimization of the molecules in the neutral state, and unrestricted formalism was used for optimization of radical cations. The electronic structures and frontier orbital energies for the neutral states of the molecules were calculated at the same level of theory. For **An-BTBT-An** and **BTBT-An-BTBT**, HOMO /LUMO energies (in a gas phase, tetrahydrofuran and acetonitrile) have also been calculated by a single-point calculations at B3LYP/G-311G(d,p) level for the geometries taken from a single crystal X-ray diffraction structures. The visualization of the orbital coefficients was performed with GaussView 6.0 software. For computational estimations of the hole mobilities, the calculations of transfer integrals and reorganization energies were performed using PW91 functional with TZ2P basis set as implemented in Amsterdam Density Functional (ADF) suite of programs.^[10]

For the estimation of hole mobility of **BTBT-An-BTBT** and **An-BTBT-An**, their structures were optimized for both neutral and radical cation states at B3LYP/6-311G(d,p) level of theory. The calculations of intermolecular transfer integrals and reorganization energies were performed by PW91 functional with the basis set of triple-Z 2plus polarization function (TZ2P) in Amsterdam Density Functional (ADF) program.

The theoretical mobility can be calculated by hopping model based on semi-classical Marcus-Hush theory. In this case, the charge carriers are localized on a single molecule and the hopping charge transfer rate constant k (for the case of self-exchange process with the total Gibbs energy $\Delta G^0 = 0$)

$$k = \frac{V^2}{\hbar} \left(\frac{\pi}{\lambda k_B T} \right)^{1/2} \exp \left(- \frac{\lambda}{4k_B T} \right)$$

is described as follow:

where k_B is the Boltzmann constant (1.38×10^{-23} J/K), \hbar is the Planck constant (1.055×10^{-34} J s/radian), T is the absolute temperature (298 K in our calculations), V is the transfer integral (electronic coupling) for electron (hole) transfer between two adjacent molecules and λ is the charge reorganization energy which is defined as the energy change associated with the geometry relaxation during the charge transfer.

In the low field limit, the carrier mobility μ can be well described by the Einstein equation:^[11,12]

$$\mu = \frac{e}{k_B T} D$$

where e is the electron charge (1.60×10^{-19} C) and D is the average diffusion coefficient of the charge starting from a molecule and towards all directions in three-dimensional spaces.

The charge motion is assumed to be a homogeneous random walk, in which case the diffusion coefficient can be evaluated from the hopping rates as:

$$D = \lim_{t \rightarrow \infty} \frac{1}{2n} \frac{\{x(t)^2\}}{t} \approx \frac{1}{2n} \sum_i r_i^2 k_i P_i = \frac{1}{2n} \frac{r_i^2 k_i^2}{\sum_i k_i}$$

where n is the dimension ($n = 3$), r_i and k_i are the distance and the charge transfer rate constant between two adjacent molecules, respectively, and P_i is the relative probability of the charge

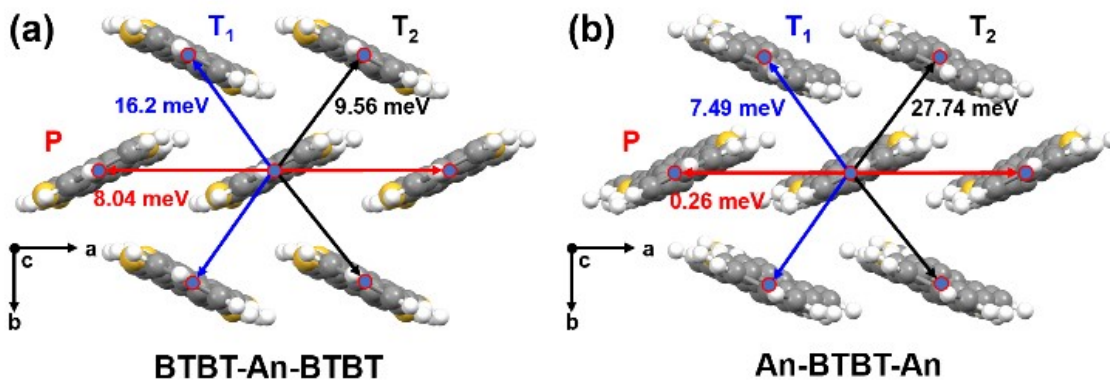
transfer in the i_{th} dimer.

Table S1. Crystal data and structure refinement parameters.

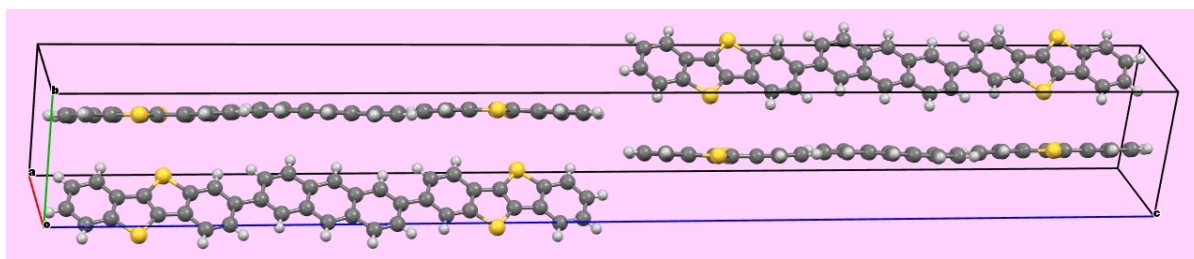
Compound	An-BTBT-An	BTBT-An-BTBT
Empirical formula	C ₄₂ H ₂₄ S ₂	C ₄₂ H ₂₂ S ₄
Formula weight	592.73	654.84
Temperature/K	293	100
Crystal system	monoclinic	monoclinic
Space group	P2 ₁ /c	P2 ₁ /c
a/Å	5.997(8)	5.9092(4)
b/Å	7.699(11)	7.7202(5)
c/Å	59.33(8)	61.940(4)
α /°	90.00	90.00
β /°	90.00	90.02
γ /°	90.00	90.00
Volume/Å ³	2739(7)	2825.7(3)
Z	4	4
$\rho_{\text{calc}}/\text{cm}^3$	1.437	1.539
μ/mm^{-1}	0.228	3.351
F(000)	1232.0	1352.0
Reflections collected	4815	5785
Independent reflections, R _{int} , R σ	1396, 	4689,
Data/restraints/parameters	1396/0/397	4689/0/415
Goodness-of-fit on F ²	1.452	1.051
R ₁ indexes [$I \geq 2\sigma(I)$]	0.1362	0.0764
wR ₂ indexes [all data]	0.4214	0.1893

Table S2 The intermolecular distances (r_i), transfer integrals (V_h), reorganization energies (λ_h) and mobilities (μ_h^{calc}) of **BTBT-An-BTBT** and **An-BTBT-An**.

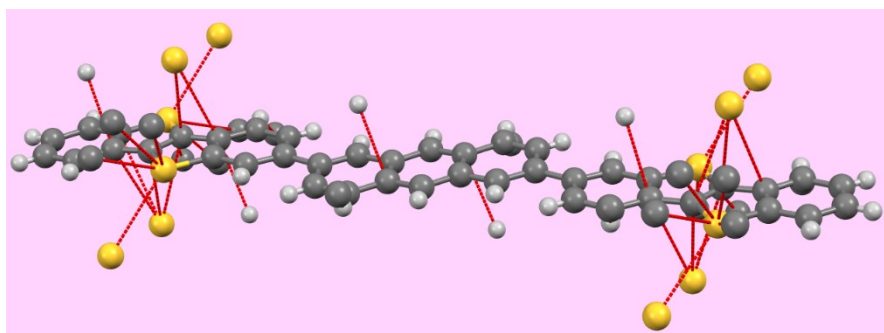
Material	Direction	r_i (Å)	V_h (meV)	λ_h (meV)	μ_h^{calc} ($\text{cm}^2 \text{V}^{-1} \text{s}^{-1}$)
BTBT-An-BTBT	P	5.909	8.04	145	0.032
	T1	4.844	16.02		
	T2	4.879	9.56		
An-BTBT-An	P	5.997	0.26	108	0.198
	T1	4.897	7.49		
	T2	4.868	27.74		



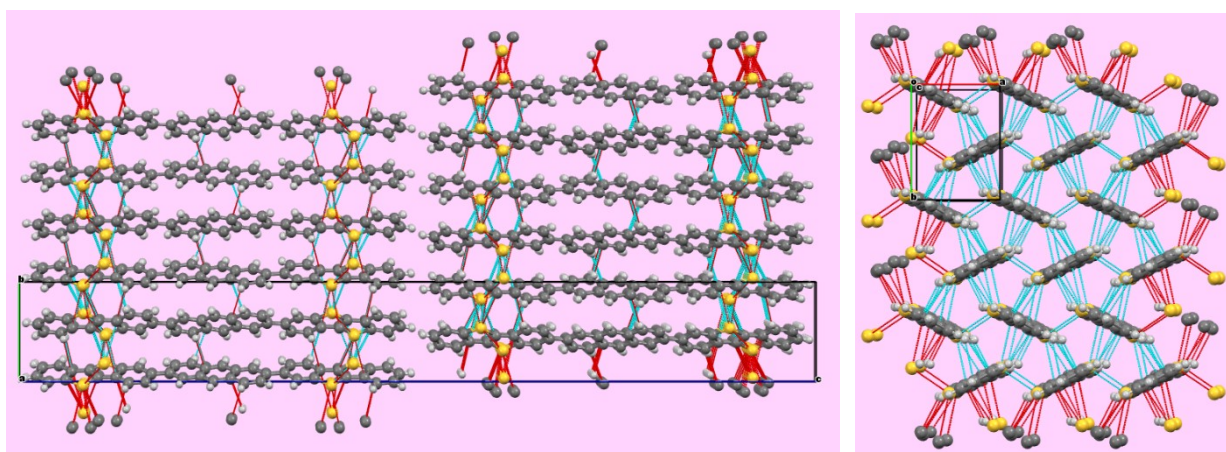
The molecular packing structures and the HOMO transfer integrals (six nearest neighbor contacts) of **BTBT-An-BTBT** (a) and **An-BTBT-An** (b) within the respective layer.



BTBT-An-BTBT in a unit cell $(a,b,c) = (1,1,1)$.



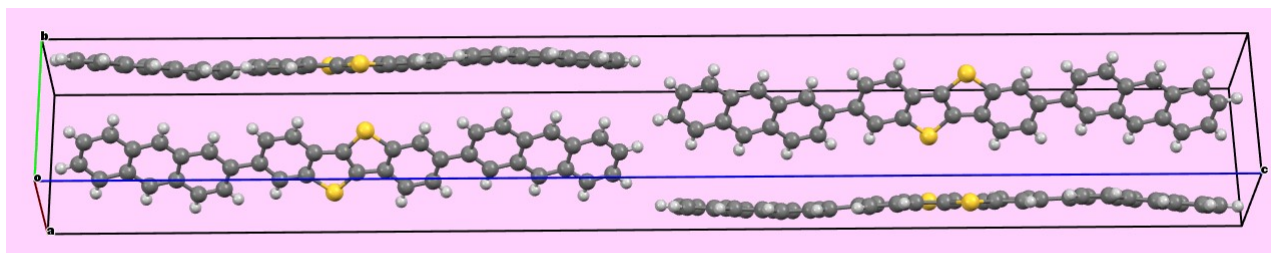
Short intermolecular contacts in **BTBT-An-BTBT**.



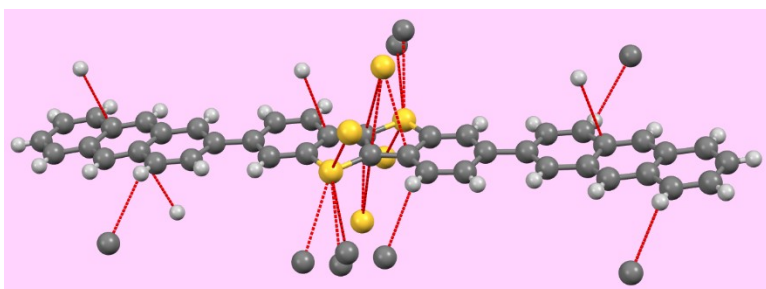
Short intermolecular contacts in **BTBT-An-BTBT** crystal.

Left: view along a-axis. $(a, b, c) = (3, 3, 1)$. Right: view along c-axis. $(a, b, c) = (3, 3, 0.5)$

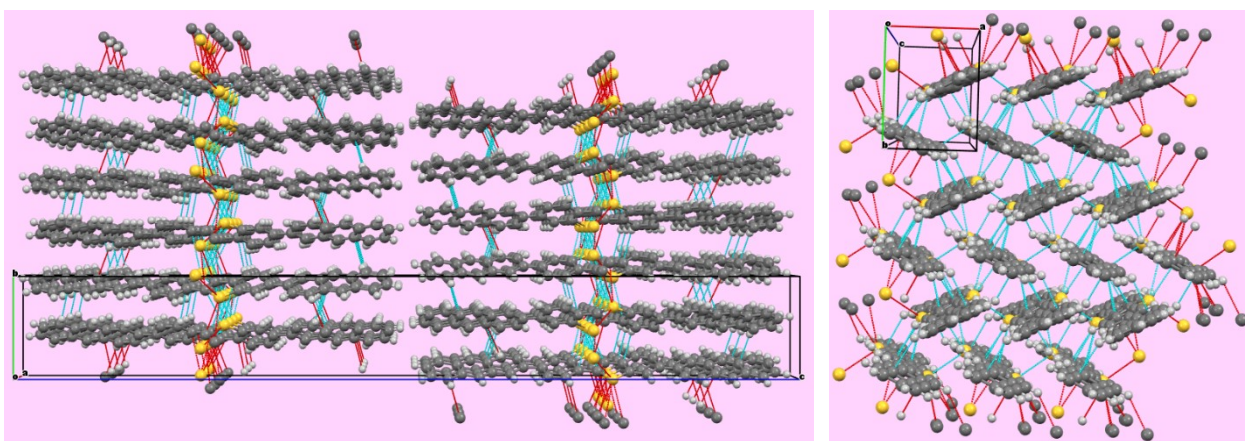
Figure S1. Molecular packing structure of **BTBT-An-BTBT**, showing short intermolecular $C\cdots H-\pi$, $S\cdots S$, $C\cdots S$, $S\cdots\pi$ contacts.



An-BTBT-An in a unit cell $(a,b,c) = (1,1,1)$.



Short intermolecular contacts in **An-BTBT-An**.



Short intermolecular contacts in **An-BTBT-An** crystal.

Left: view along a-axis. $(a, b, c) = (3, 3, 1)$. Right: view along c-axis. $(a, b, c) = (3, 3, 0.5)$

Figure S2. Molecular packing structure of **An-BTBT-An**, showing short intermolecular $C\cdots H-\pi$, $S\cdots S$, $C\cdots S$, $S\cdots \pi$ contacts.

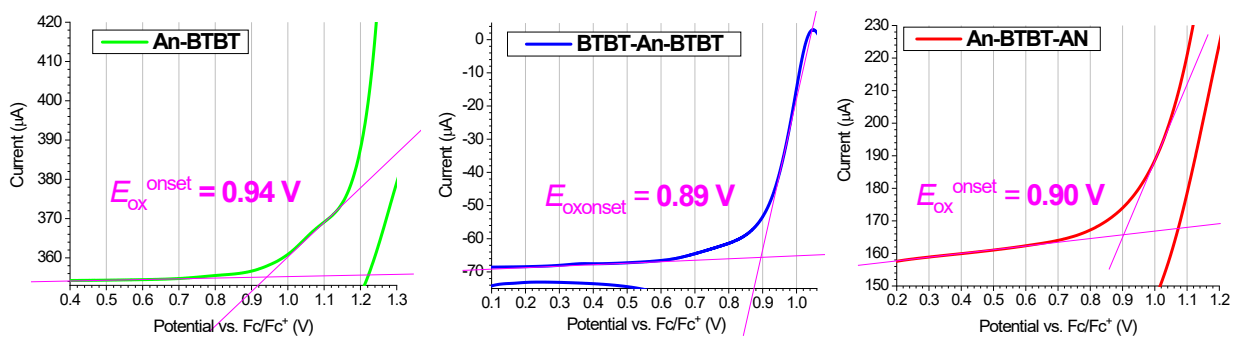


Figure S3. Expanded regions of cyclic voltammograms (Figure 2a) for estimation of E_{ox}^{onset} values of studied compounds. CV of vacuum-deposited films on glassy carbon electrode (GCE, $d = 3$ mm) in 0.1 M Bu_4NPF_6 / CH_3CN , scan rate 20 mV/s.

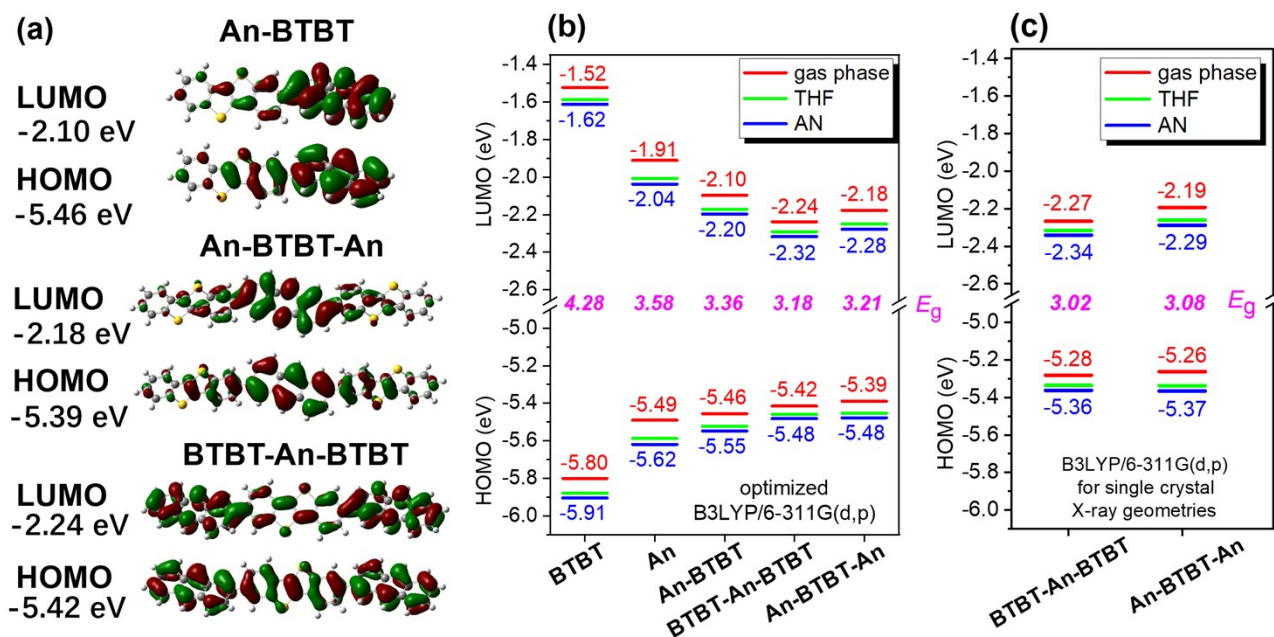


Figure S4. (a) HOMO and LUMO distribution in An-BTBT, BTBT-An-BTBT and An-BTBT-An from B3LYP/6-311G(d,p) calculations in a gas phase. (b) HOMO and LUMO energies for B3LYP/6-311G(d,p) optimized geometries of BTBT, anthracene, An-BTBT, BTBT-An-BTBT and An-BTBT-An in a gas phase, and (with a PCM model) in tetrahydrofuran and acetonitrile. (c) HOMO and LUMO energies from B3LYP/6-311G(d,p) single point calculations at the geometries taken from single crystal X-ray diffraction experiments (in a gas phase, THF and AN). For (b,c), the HOMO–LUMO energy gaps (E_g) are shown for a gas phase (in magenta).

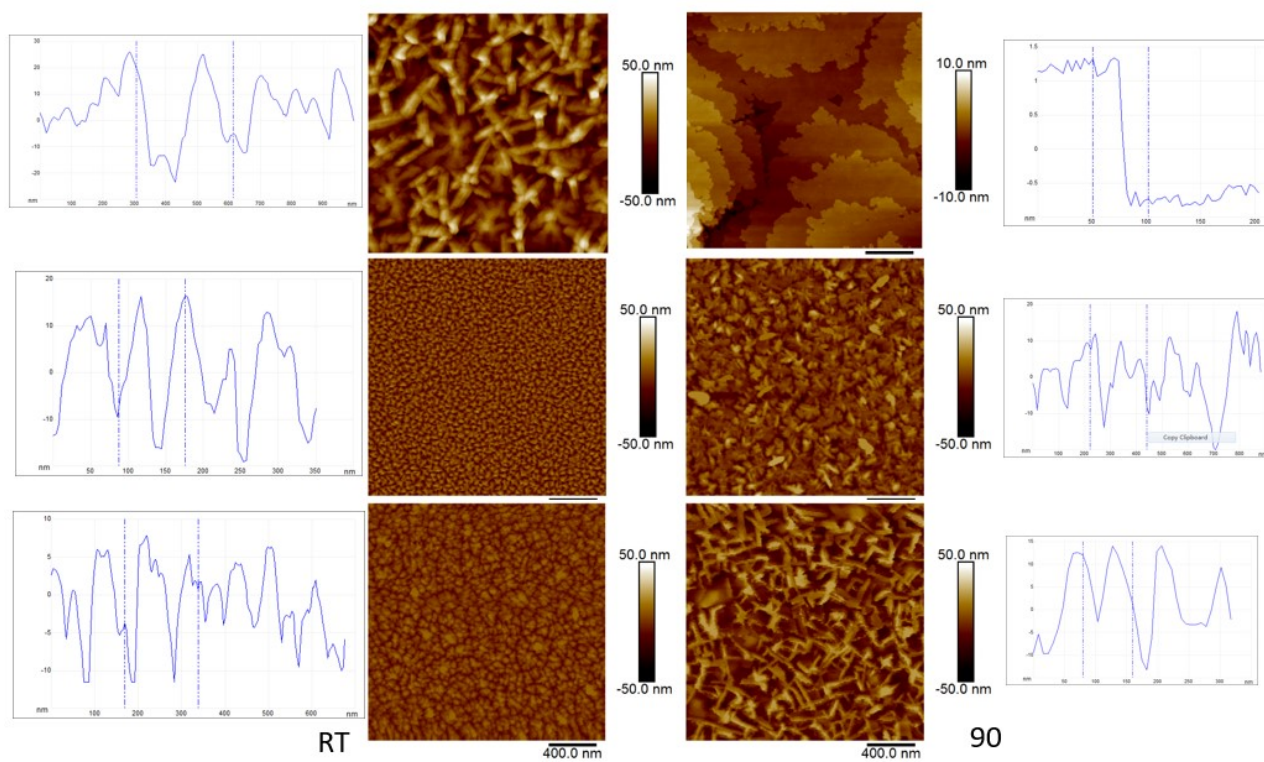


Figure S5. AFM images of thin films of three compounds (from top to bottom: **An-BTBT**, **BTBT-An-BTBT** and **An-BTBT-An**, respectively) deposited on OTS-treated wafer substrate at both 20 °C (left) and at 90 °C (right).

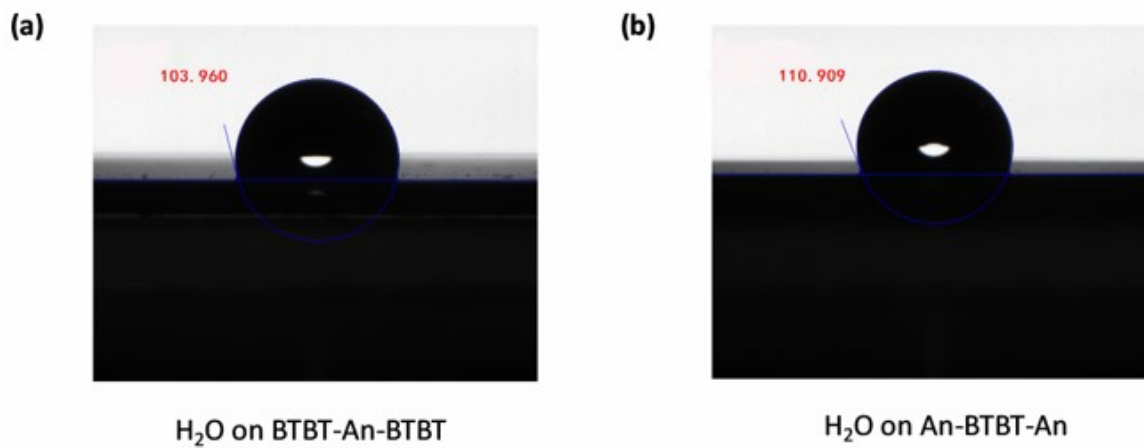


Figure S6. The contact angles of water on the surface of (a) **BTBT-An-BTBT** and (b) **An-BTBT-An** thin films are 104° and 111°, respectively.

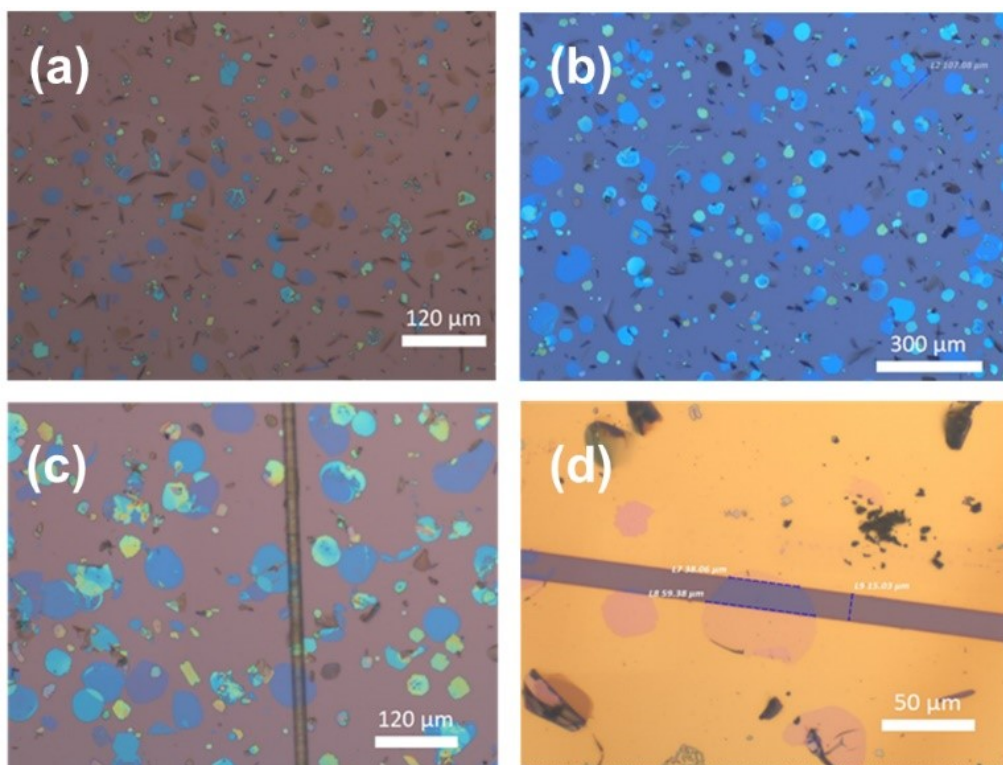


Figure S7. Polarizing optical microscopy (POM) images of **BTBT-An-BTBT** (a) and **An-BTBT-An** (b) single crystals. POM images of a single crystal OFET fabricated with ultrathin wire (d ~15 μm) before (c) and after (d) the evaporation of gold source and drain electrodes.

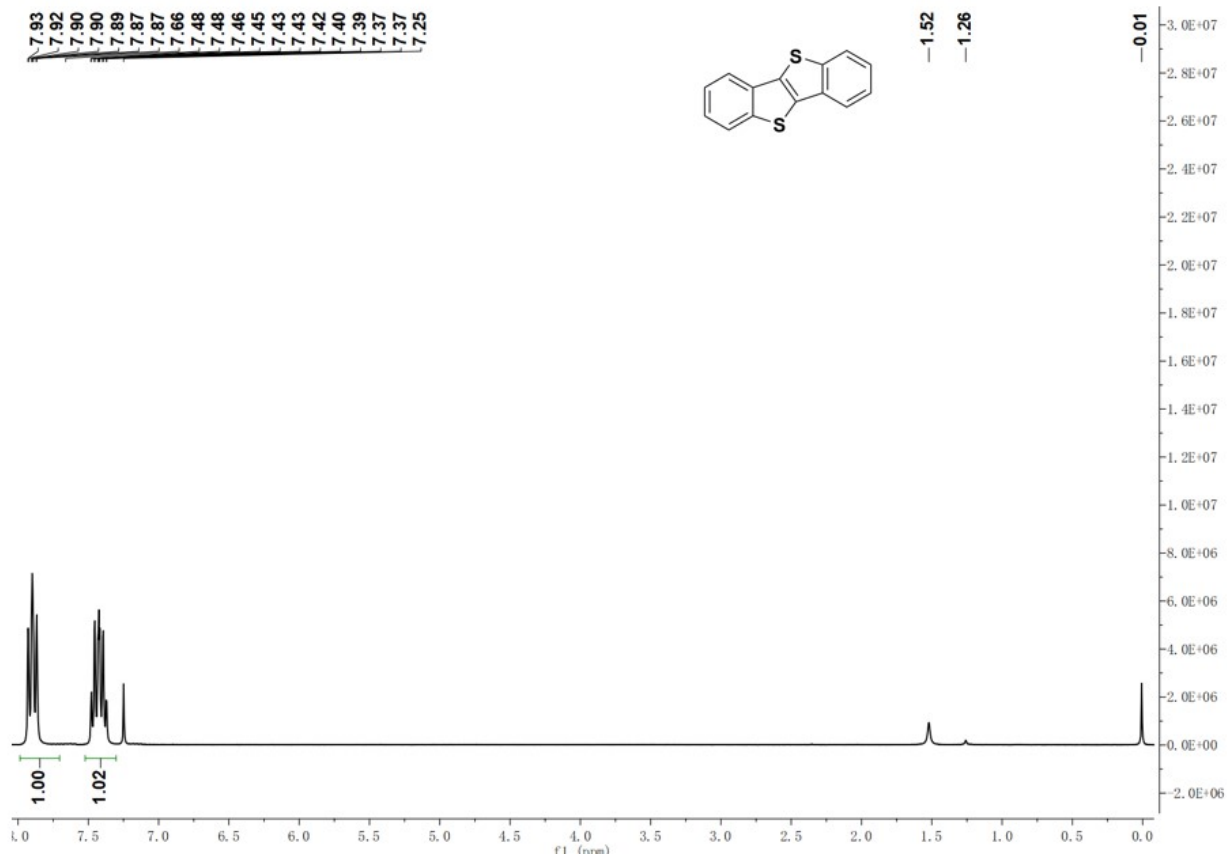


Figure S8. ¹H NMR spectrum of BTBT.

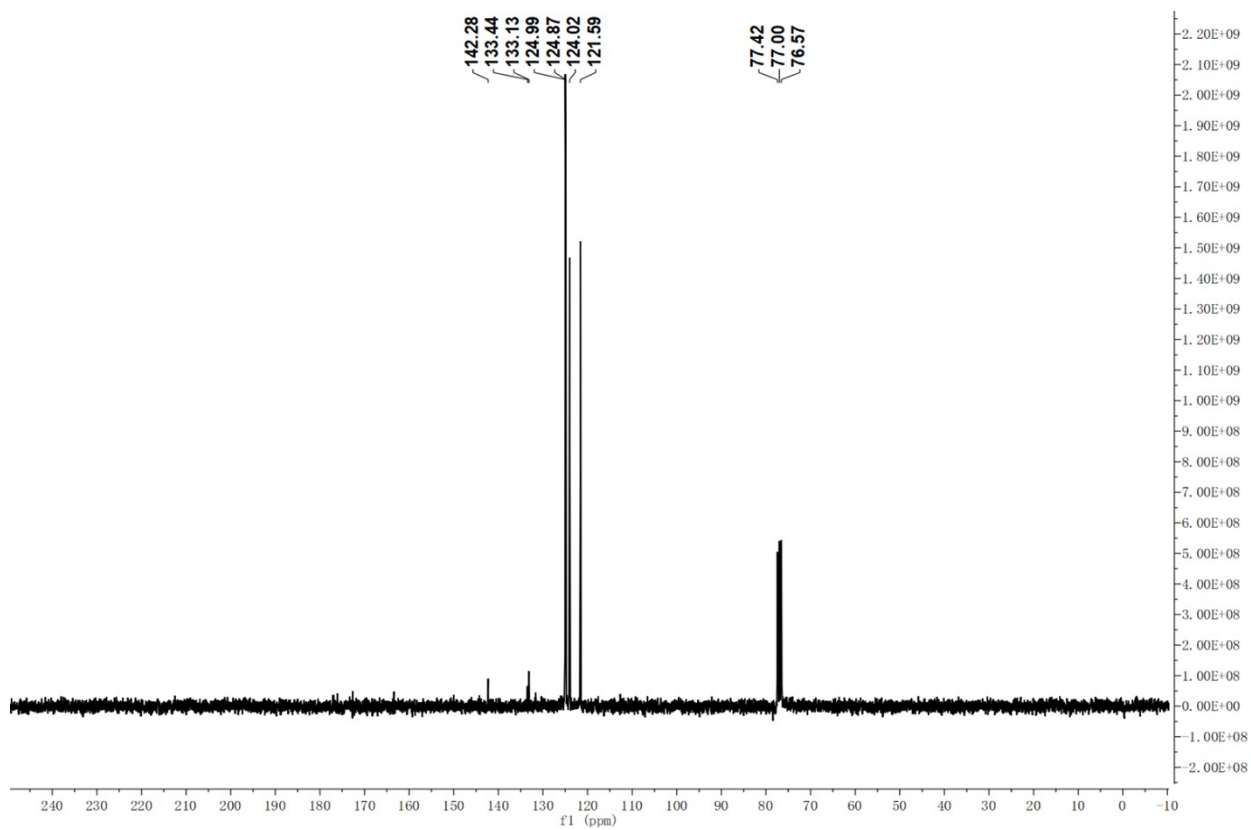


Figure S9. ¹³C NMR spectrum of BTBT (2).

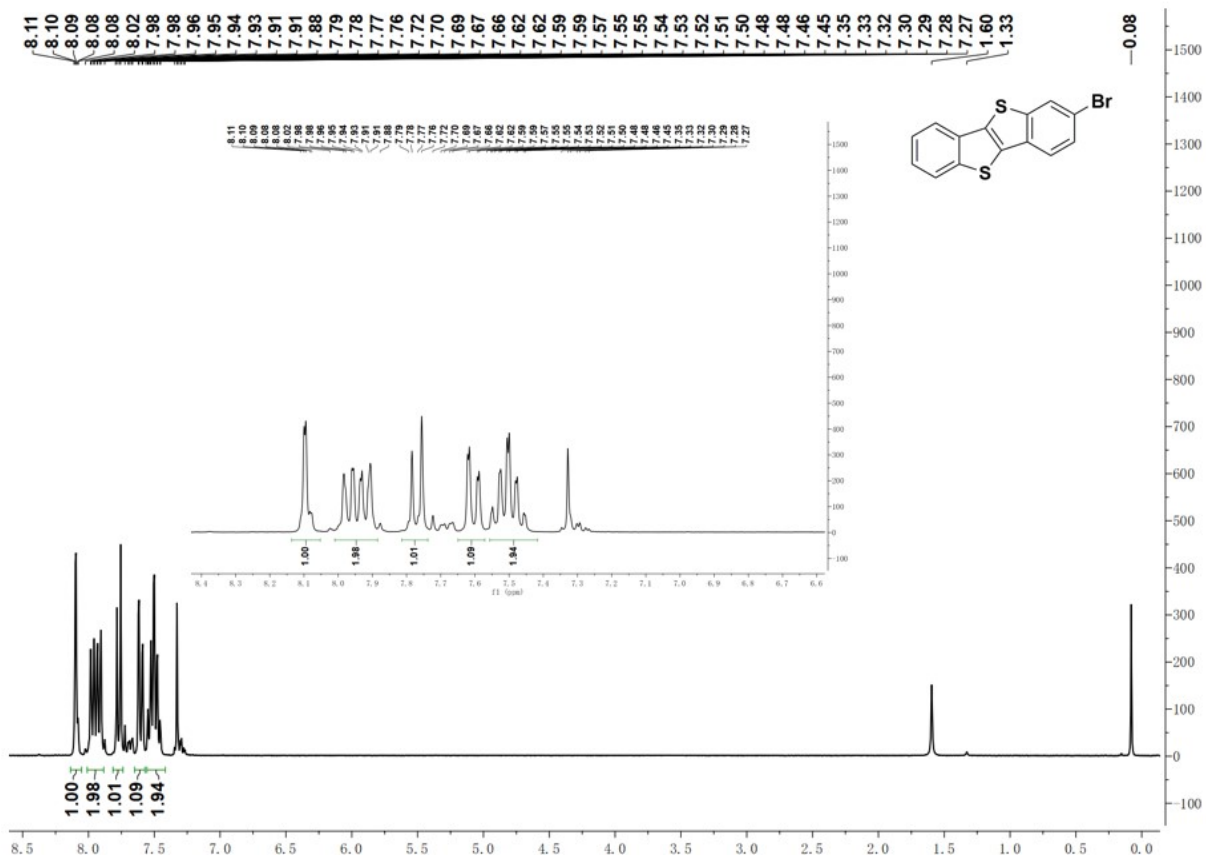


Figure S10. ^1H NMR spectrum of 2-bromo-BTBT (3).

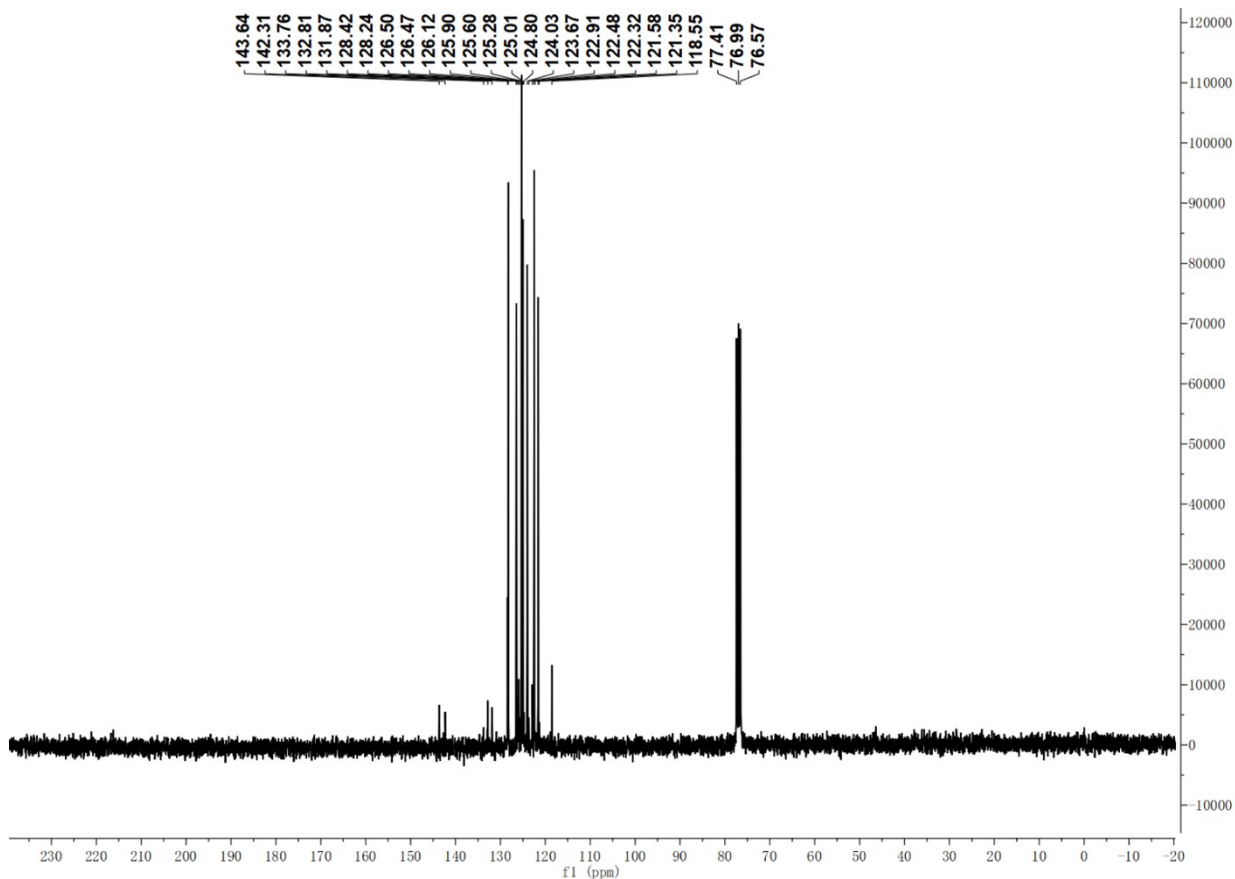


Figure S11 ^{13}C NMR spectrum of 2-bromo-BTBT (3).

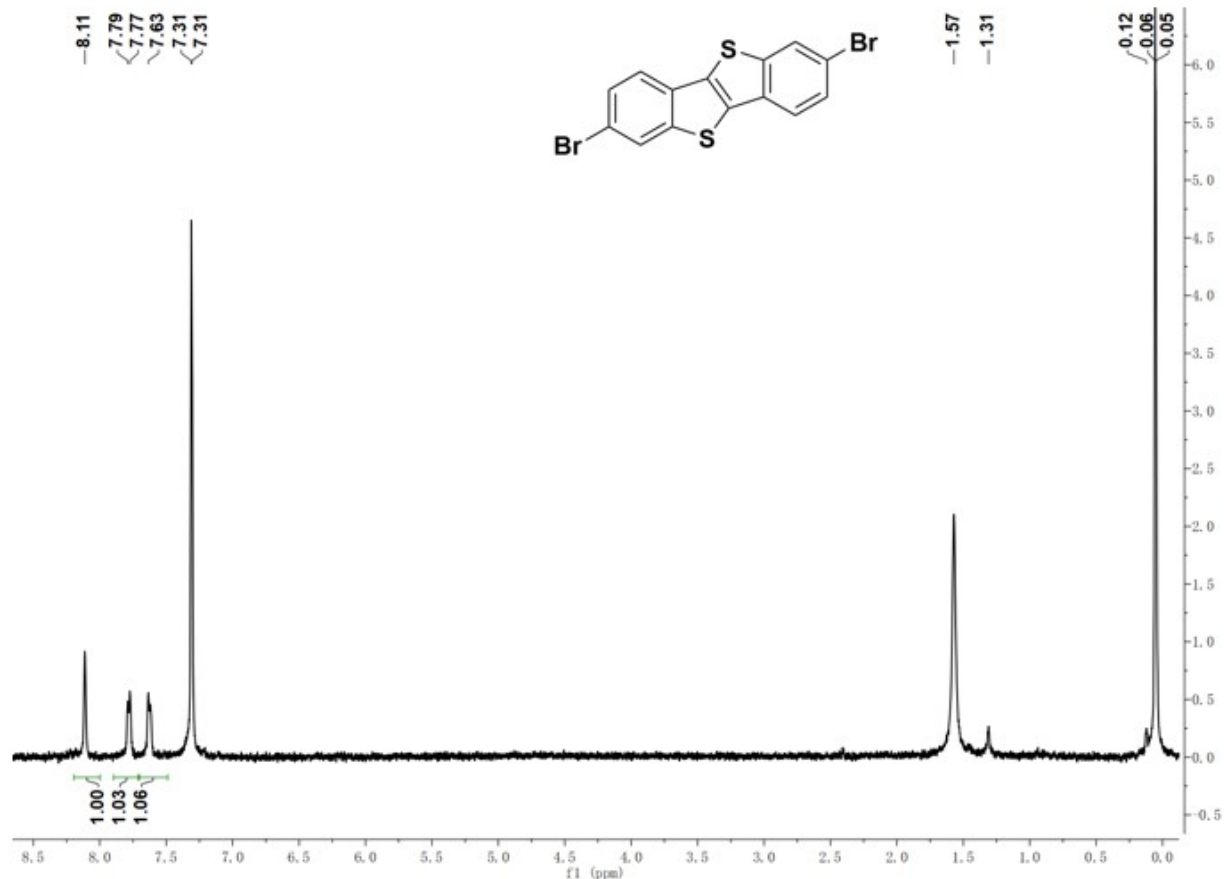


Figure S12. ¹H NMR spectrum of 2,7-dibromo-BTBT (7).

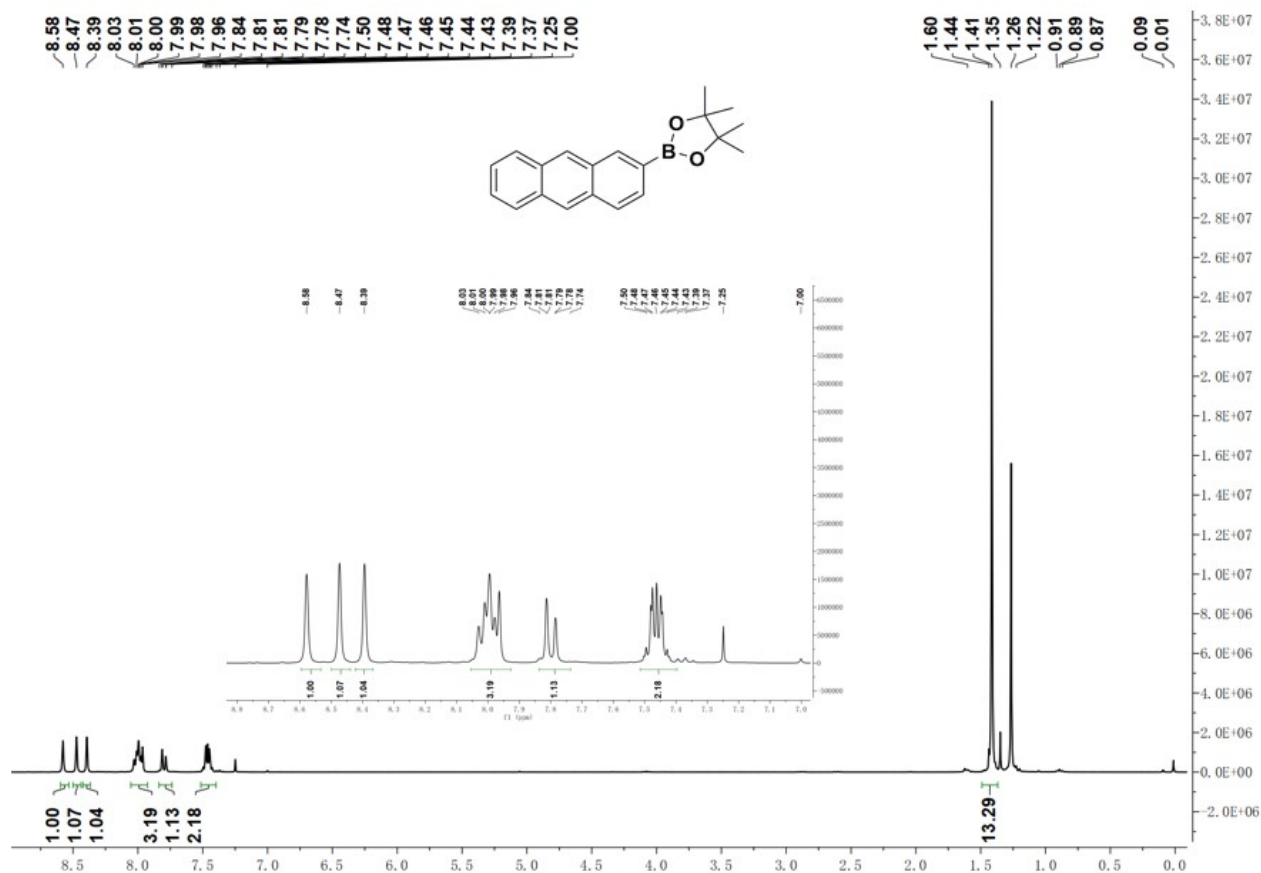


Figure S13. ¹H NMR spectrum of 2-(anthracen-2-yl)-4,4,5,5-tetramethyl-1,3,2-dioxaborolane (9).

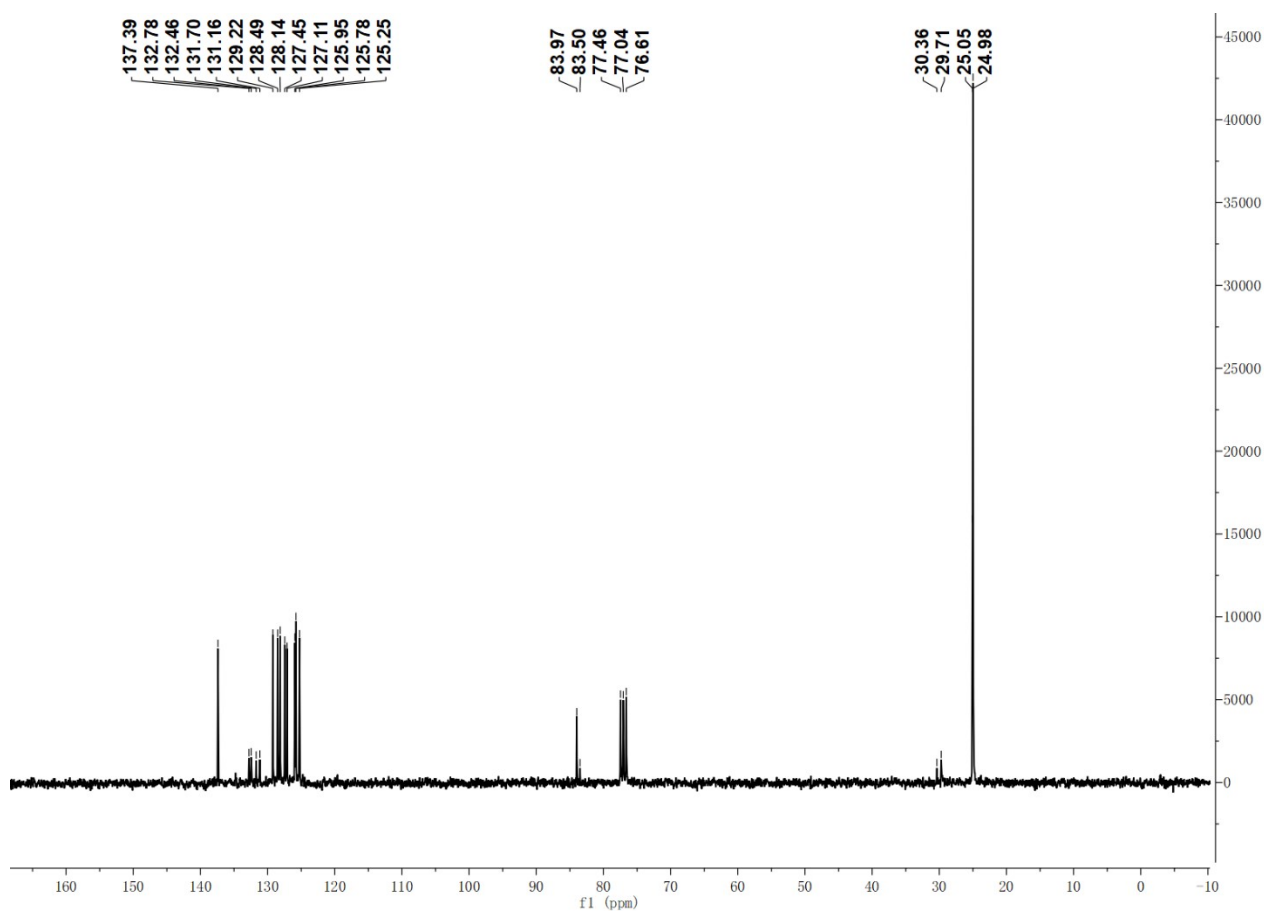


Figure S14. ^{13}C NMR spectrum of 2-(anthracen-2-yl)-4,4,5,5-tetramethyl-1,3,2-dioxaborolane (**9**).

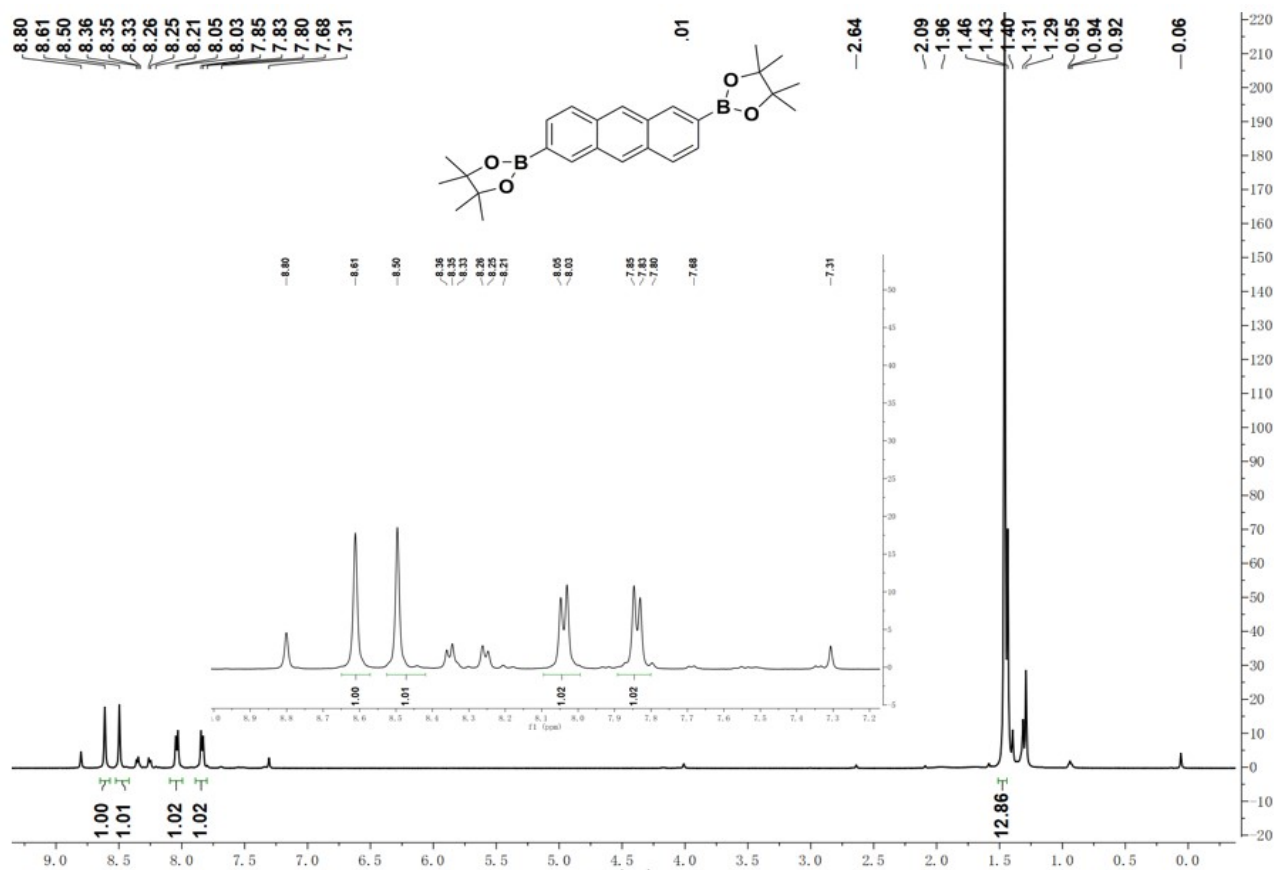


Figure S15. ^1H NMR spectrum of 2,6-bis(4,4,5,5-tetramethyl-1,3,2-dioxaborolan-2-yl)-anthracene

(11).

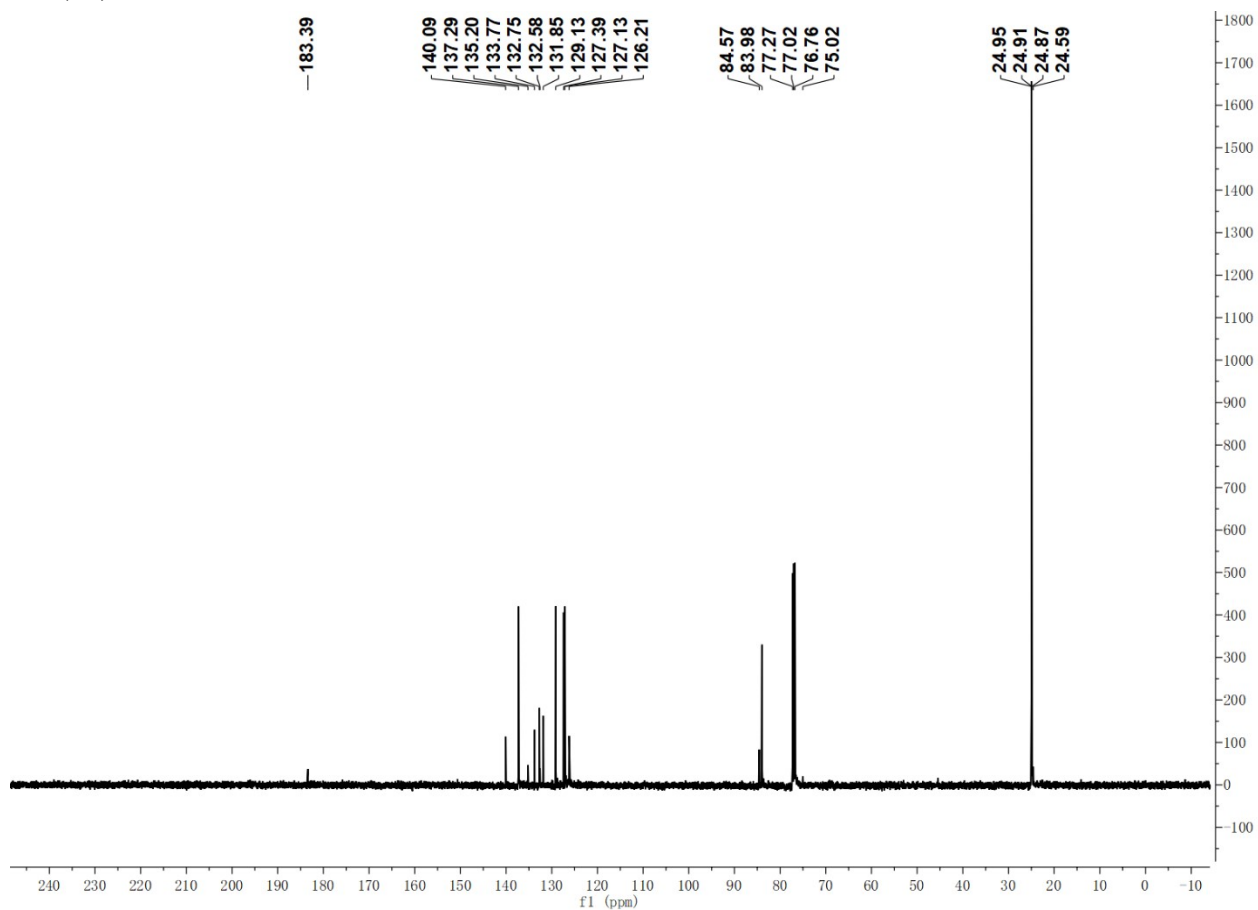


Figure S16. ¹³C NMR spectrum of 2,6-bis(4,4,5,5-tetramethyl-1,3,2-dioxaborolan-2-yl)-anthracene (11).

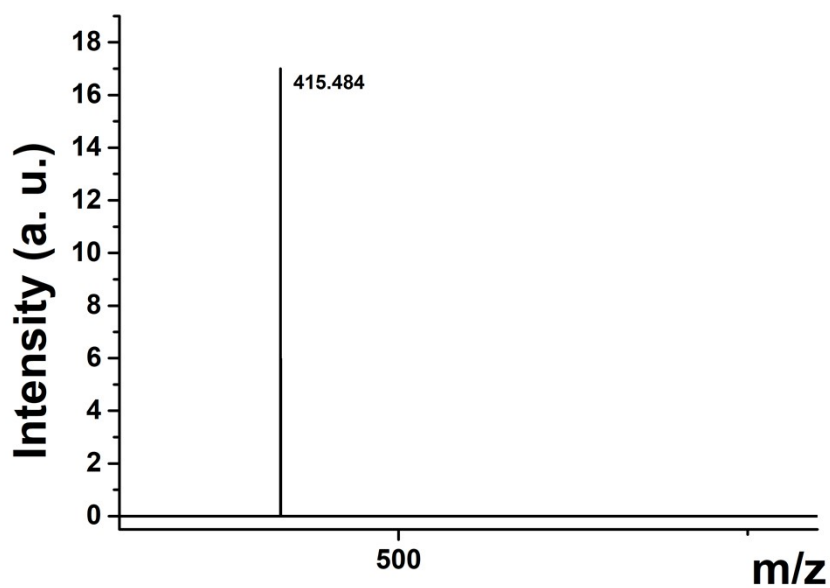


Figure S17. MALDI-TOF mass-spectrum of An-BTBT.

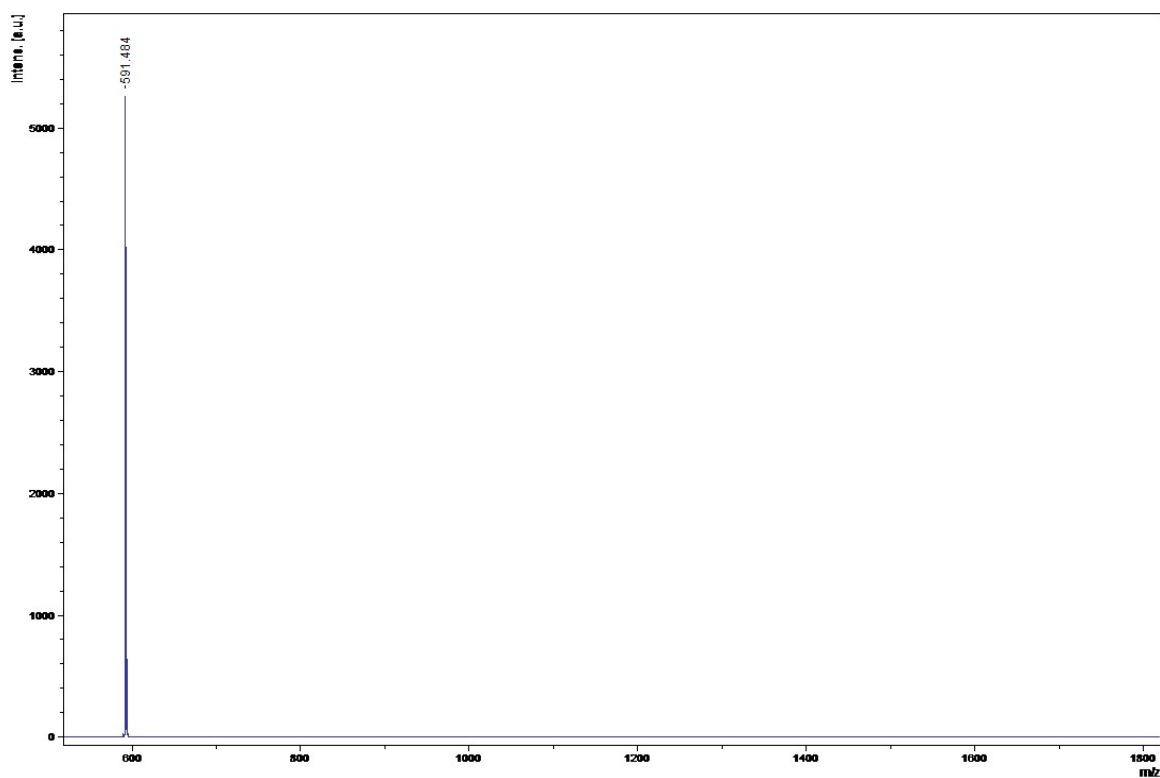


Figure S18. MALDI-TOF mass-spectrum of An-BTBT-An.

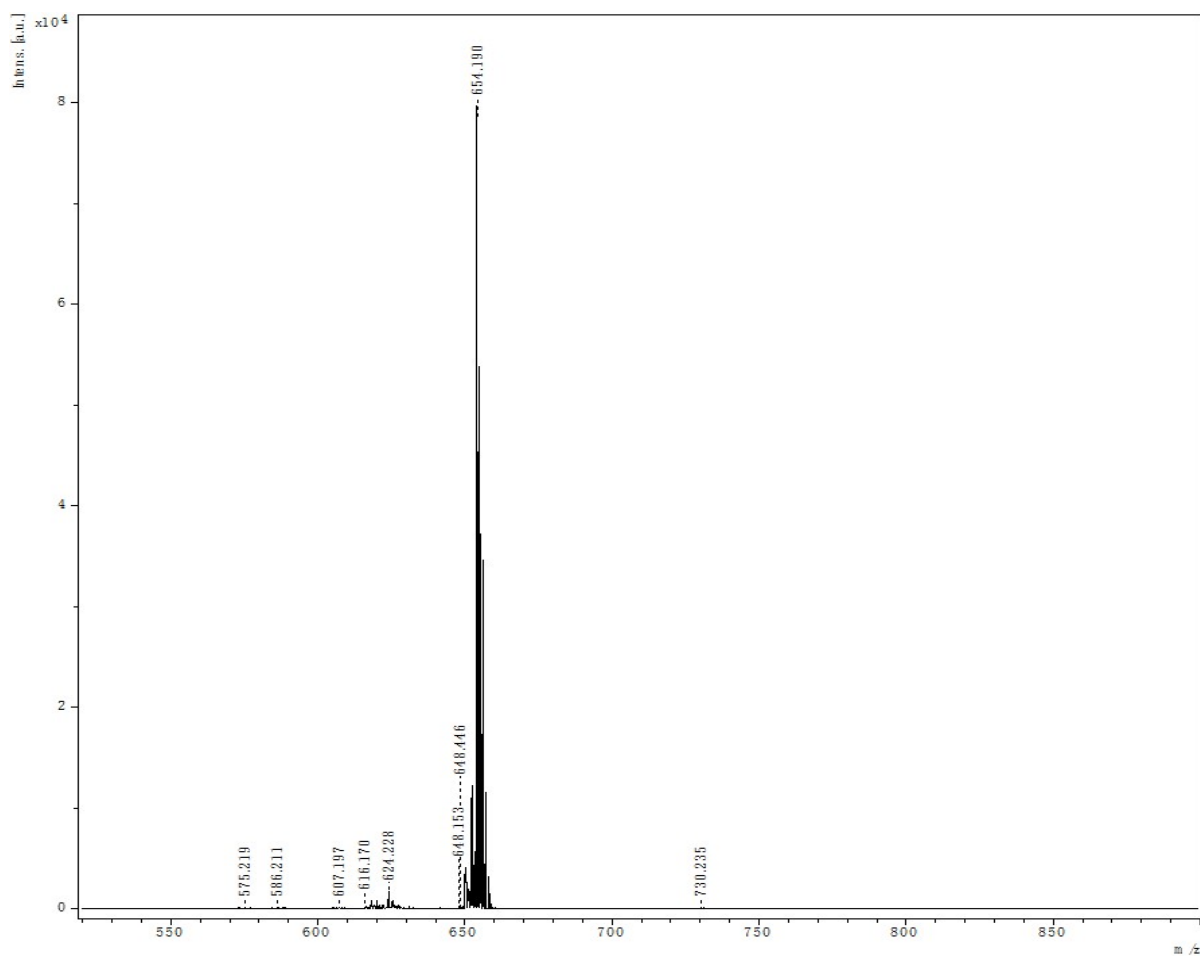


Figure S19. MALDI-TOF mass-spectrum of BTBT-An-BTBT.

References

- [1] M. Saito, I. Osaka, E. Miyazaki, K. Takimiya, H. Kuwabara, and M. Ikeda, One-step Synthesis of [1]Benzothieno[3,2-b][1]benzothiophene from o-Chlorobenzaldehyde. *Tetrahedron Lett.*, **2011**, 52, 285–288.
- [2] S. Inoue, H. Minemawari, J. Tsutsumi, M. Chikamatsu, T. Yamada, S. Horiuchi, M. Tanaka, R. Kumai, M. Yoneya, and T. Hasegawa, Effects of Substituted Alkyl-Chain Length on Solution-Processable Layered Organic Semiconductor Crystals. *Chem. Mater.*, **2015**, 27, 3809–3812.
- [3] R. J. Griffith, Polymeric organic semiconductor compositions. Patent WO2015/028768 EN 2015.03.05.
- [4] H. Meng, F. Sun, M. B. Goldfinger, G. D. Jaycox, Z. Li, W. J. Marshall, and G. S. Blackman, High-Performance, Stable Organic Thin-Film Field-Effect Transistors Based on Bis-5'-alkylthiophen-2'-yl-2,6-anthracene Semiconductors. *J. Am. Chem. Soc.*, **2005**, 127, 2406–2407.
- [5] V. Coropceanu, J. Cornil, D. A. da Silva Filho, Y. Olivier, R. Silbey, and J.-L. Brédas, Charge Transport in Organic Semiconductors, *Chem. Rev.*, **2007**, 107, 926–952.
- [6] Agilent Technologies, CrysAlisPRO, Version 1.171.36.28, 2013.
- [7] O. V. Dolomanov, L. J. Bourhis, R. J. Gildea, J. A. K. Howard, H. Puschmann, OLEX2: a complete structure solution, refinement and analysis program. *J. Appl. Cryst.*, **2009**, 42, 339–341.
- [8] D. Kratzert, J. J. Holstein, I. Krossing, DSR: enhanced modelling and refinement of disordered structures with SHELXL. *J. Appl. Cryst.*, **2015**, 48, 933–938.
- [9] Gaussian 16, Revision A.03, M. J. Frisch, G. W. Trucks, H. B. Schlegel, G. E. Scuseria, M. A. Robb, J. R. Cheeseman, G. Scalmani, V. Barone, G. A. Petersson, H. Nakatsuji, X. Li, M. Caricato, A. V. Marenich, J. Bloino, B. G. Janesko, R. Gomperts, B. Mennucci, H. P. Hratchian, J. V. Ortiz, A. F. Izmaylov, J. L. Sonnenberg, D. Williams-Young, F. Ding, F. Lipparini, F. Egidi, J. Goings, B. Peng, A. Petrone, T. Henderson, D. Ranasinghe, V. G. Zakrzewski, J. Gao, N. Rega, G. Zheng, W. Liang, M. Hada, M. Ehara, K. Toyota, R. Fukuda, J. Hasegawa, M. Ishida, T. Nakajima, Y. Honda, O. Kitao, H. Nakai, T. Vreven, K. Throssell, J. A. Montgomery, Jr., J. E. Peralta, F. Ogliaro, M. J. Bearpark, J. J. Heyd, E. N. Brothers, K. N. Kudin, V. N. Staroverov, T. A. Keith, R. Kobayashi, J. Normand, K. Raghavachari, A. P. Rendell, J. C. Burant, S. S. Iyengar, J. Tomasi, M. Cossi, J. M. Millam, M. Klene, C. Adamo, R. Cammi, J. W. Ochterski, R. L. Martin, K. Morokuma, O. Farkas, J. B. Foresman, and D. J. Fox, Gaussian, Inc., Wallingford CT, 2016.
- [10] Amsterdam Density Functional (ADF), Users Guide, Release 1.1; Department of Theoretical Chemistry, Free University, Amsterdam, The Netherlands, 1994.
<https://www.scm.com/>
- [11] V. Coropceanu, J. Cornil, D. A. da Silva Filho, Y. Olivier, R. Silbey, J.-L. Brédas, Charge transport in organic semiconductors. *Chem. Rev.*, **2007**, 107, 926-952.
- [12] L. Wang, G. Nan, X. Yang, Q. Peng, Q. Li, Z. Shuai, Computational methods for design of organic materials with high charge mobility. *Chem. Soc. Rev.*, **2010**, 39, 423-434.